

## Test of constancy of speed of light with rotating cryogenic optical resonators

P. Antonini, M. Okhapkin, E. Göklü,\* and S. Schiller

*Institut für Experimentalphysik, Heinrich-Heine-Universität Düsseldorf, 40225 Düsseldorf, Germany*

(Received 23 July 2004; revised manuscript received 7 April 2005; published 25 May 2005)

A test of Lorentz invariance for electromagnetic waves was performed by comparing the resonance frequencies of two optical resonators as a function of orientation in space. In terms of the Robertson-Mansouri-Sexl theory, we obtain  $\beta - \delta - 1/2 = (+0.5 \pm 3 \pm 0.7) \times 10^{-10}$ , a tenfold improvement compared to the previous best results. We also set a first upper limit for a parameter of the standard model extension test theory,  $|(\tilde{\kappa}_{e-})^{ZZ}| < 2 \times 10^{-14}$ .

DOI: 10.1103/PhysRevA.71.050101

PACS number(s): 03.30.+p, 12.60.-i, 07.60.-j

### I. INTRODUCTION

The principle of local Lorentz invariance (LLI), stating the independence of physical laws from the state of motion of inertial laboratories, is one of the most fundamental facts about our physical world. An early precision measurement, demonstrating LLI for light propagation, was performed by Michelson and Morley in 1887 and its result was an essential experimental foundation for the advent of relativity. LLI is incorporated as a fundamental symmetry into the accepted theories of the fundamental forces, general relativity [1] and the standard model. Numerous experiments have tested LLI with respect to matter and to the electromagnetic field, and have upheld its validity [2]. For electromagnetic waves the isotropy of space has so far been verified at the level of a few parts in  $10^{15}$  [3–7].

New generations of tests of LLI and of other fundamental symmetries [weak equivalence principle, local position invariance, charge-parity-time (CPT) Symmetry] are seen as important approaches in the quest for a deeper understanding of the forces of nature [2]. They might provide useful input for the development of a theory able to describe gravity at the quantum level. In these theories, violations of fundamental symmetries are being considered. Thus, the theoretical models call for improved experiments to either validate LLI at much higher precision levels, or to uncover its limits of validity.

Violations of LLI can be interpreted using so-called test theories. A kinematic test theory commonly applied is that by Robertson, Mansouri, and Sexl (RMS) [8]. Here, light propagation is described relative to a preferred frame (“ether frame”)  $\Sigma$  in which there is no preferred direction and thus the speed of light  $c_0$  is constant. Usually the frame in which the cosmic microwave background is isotropic is assumed to be this frame. Lorentz transformations between a laboratory frame  $S$  and  $\Sigma$  are replaced by general linear transformations that depend on the velocity  $\vec{v}$  of the lab frame with respect to  $\Sigma$  and on three phenomenological parameters  $\alpha$ ,  $\beta$ , and  $\delta$ . These reduce to  $\alpha = -\frac{1}{2}$ ,  $\beta = \frac{1}{2}$ ,  $\delta = 0$  if LLI is valid. In the moving frame  $S$ , the speed of light can be expressed to low-

est order in  $|\vec{v}|/c_0$  as  $c(\phi, v)/c_0 = 1 + (v^2/c_0^2)[\beta - \alpha - 1 + (\frac{1}{2} - \beta + \delta)\sin^2\phi]$ , where  $\phi$  is the angle of the direction of light propagation relative to the velocity  $\vec{v}$  of the laboratory. Thus, violations of the constancy of the speed of light are described by two nonzero parameter combinations.

Recently, a comprehensive dynamical test theory of LLI violation has been developed, the standard model extension (SME) [9]. It is based on the Lagrangian of the standard model, extended by terms that violate LLI and CPT. These terms describe possible violations in the behavior of both matter and fields, and contain a large number of unknown parameters, whose values can in principle be determined by an appropriately large set of (partially independent) experiments. In particular, the extended Lagrangian of the electromagnetic field is given by  $\mathcal{L} = -\frac{1}{4}F_{\mu\nu}F^{\mu\nu} - \frac{1}{4}(k_F)_{\kappa\lambda\mu\nu}F^{\kappa\lambda}F^{\mu\nu}$ . The dimensionless tensor  $(k_F)_{\kappa\lambda\mu\nu}$  describes violations of LLI and has 19 independent coefficients. Its values are dependent on the frame of reference; a frame in which the sun is stationary is chosen for practical reasons. Of these coefficients, 10 describe polarization-dependent effects. These can be restricted to the level of  $10^{-32}$  using astronomical observations of the polarization of distant light sources [10].

Of the remaining nine coefficients, one ( $\tilde{\kappa}_{lr}$ ) describes an asymmetry of the one-way speed of electromagnetic waves [11], while the others describe different aspects of violations of constancy, i.e., a dependence on propagation direction and on the speed of the laboratory frame of reference. The corresponding eight coefficients can be arranged in two traceless  $3 \times 3$  matrices: the antisymmetric  $(\tilde{\kappa}_{o+})^{ij}$  that describes violation of boost invariance and therefore enters observable quantities weighted by the ratio  $\beta_{\oplus} \approx 10^{-4}$  of Earth’s orbital velocity and the speed of light, and the symmetric  $(\tilde{\kappa}_{e-})^{ij}$  quantifying anisotropy of  $c$ .

These eight coefficients can in principle be determined by measuring the time dependence of the resonance frequency of an electromagnetic resonator (assuming that particles satisfy LLI). If the electromagnetic resonator is stationary, seven coefficients can be determined by taking advantage of the rotation and orbital motion of Earth. Three experiments, using ultrastable cryogenic resonators for microwaves and optical waves, have been performed recently along this line. Lipa *et al.* [5] took data for  $\sim 100$  days and could constrain four coefficients of  $\tilde{\kappa}_{e-}$  and four linear combinations of three coefficients of  $\tilde{\kappa}_{o+}$ . Müller *et al.* [6] performed an experiment

\*Present address: ZARM, University of Bremen, 28359 Bremen, Germany.

where the measurement duration was extended to a sufficient duration (over 1 year) that the measurement of the seven coefficients was achieved. Wolf *et al.* [7] extended the measurement time further and improved significantly on the limits.

The eighth coefficient,  $(\tilde{\kappa}_{e-})^{ZZ}$ , has so far not been reported.

## II. METHOD

The resonator frequency measurement involved in a test of LLI requires a frequency reference with a frequency instability comparable to the desired measurement accuracy [4,7]. An alternative approach is the use of two cavities oriented at right angles [5,6]. One then measures the difference between the two cavity frequencies,  $\nu_1(t) - \nu_2(t)$ . For a two-cavity configuration, the beat frequency modulation can be expressed as

$$\frac{\delta(\nu_1(t) - \nu_2(t))}{\nu} = 2B(t)\sin 2\theta(t) + 2C(t)\cos 2\theta(t), \quad (1)$$

where  $\nu_1 \approx \nu_2 \approx \nu$  ( $2.8 \times 10^{14}$  Hz) is the average frequency and  $\theta(t)$  is the angle between one cavity's axis relative to the south direction. Each amplitude  $2B(t)$  and  $2C(t)$  is a linear combination of eight SME coefficients weighted by time-harmonic factors. The amplitude  $B(t)$  contains frequency components at  $0$ ,  $\omega_{\oplus}$ ,  $2\omega_{\oplus}$ ,  $\omega_{\oplus} \pm \Omega_{\oplus}$ , and  $2\omega_{\oplus} \pm \Omega_{\oplus}$ , while  $C(t)$  contains, in addition, one component at the frequency  $\Omega_{\oplus}$ . Here  $\omega_{\oplus}$  is Earth's sidereal angular frequency and  $\Omega_{\oplus}$  is Earth's orbital frequency. The determination of the individual  $\tilde{\kappa}_{o+}$  coefficients requires the ability to resolve the contribution of Earth's orbital motion in order to discriminate between frequency coefficients differing by  $\Omega_{\oplus}$ . Thus a measurement extending over of at least 1 year is necessary.

The contribution of  $(\tilde{\kappa}_{e-})^{ZZ}$  to the beat frequency signal is

$$\frac{\delta(\nu_1(t) - \nu_2(t))}{\nu} = \frac{3}{4}(\tilde{\kappa}_{e-})^{ZZ} \sin^2 \chi \cos 2\theta(t) + \dots, \quad (2)$$

where  $\chi$  is the colatitude of the laboratory.

It is evident from Eq. (2) that  $(\tilde{\kappa}_{e-})^{ZZ}$  particular Lorentz-violating coefficient is only measurable by active rotation. Another advantage is that the apparatus has to be stable only over individual rotation periods, in contrast to stationary experiments, which must be stable over 12 h. Slow (compared to the rotation period) systematic variations of the beat frequency can be eliminated in the data analysis by fitting individual rotation periods. Furthermore, in a nonrotating experiment four data values can be obtained from a measurement lasting 12 h.

In contrast, a rotating experiment offers the possibility to determine two data points  $B(t_i)$  and  $C(t_i)$  for every rotation ( $t_i$  is the midtime of the rotation period, and the period is chosen much smaller than 12 h). Thus, a rotating experiment offers a significant increase in data acquisition rate and thus a reduction of statistical noise. An overall measurement time of 1 yr or longer is still necessary for a precise determination of individual coefficients.

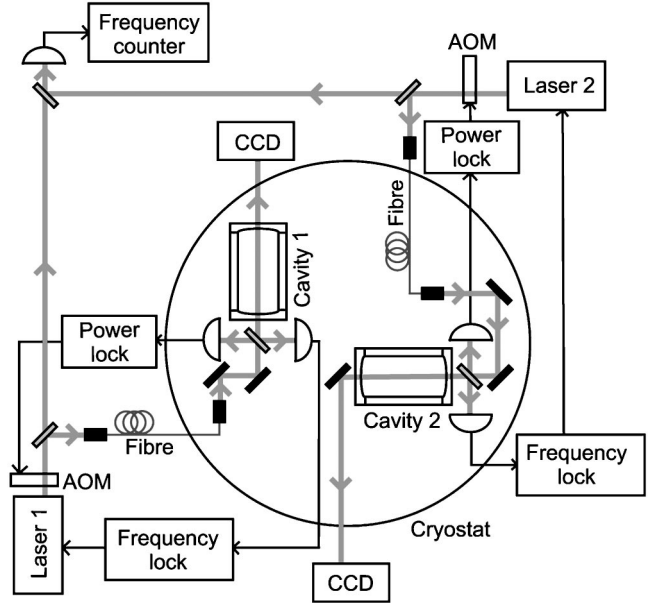


FIG. 1. The experimental setup. Two Nd:YAG lasers are frequency locked to two sapphire optical cavities located in a cryostat. The beams are fed to the resonators via optical fibers. The cavities' modes can be observed by means of two charge-coupled device cameras. Acousto-optic modulators (AOM) stabilize the power of the beams fed to the resonators. All components shown are mounted on a rotating table.

## III. EXPERIMENTAL APPARATUS

Crystalline sapphire optical cavities operated at cryogenic temperature were used. These cavities have previously been used to test LLI with a nonrotating setup [6] as well as local position invariance [12]. Figure 1 shows a schematic of the experiment. A mechanical rotation stage carries the cryostat (containing the cavities), an associated optical breadboard and most components (lasers, power supplies, servo systems). The rotation stage itself rests on an optical table that was not floated. The cavities were cooled to 3.4 K by means of a pulse-tube cooler (PTC) [13], in which He gas is periodically compressed and expanded. The use of a mechanical cooler has the advantage of continuous operation without the need to periodically refill cryogenics. Furthermore, slow mechanical deformations occurring in conventional cryostats as a consequence of change in cryogen levels are avoided.

Inside the cryostat vacuum, the two cavities together with various optical components and photodiodes were mounted on a copper base plate that was supported by rods extending from the top flange of the cryostat. Copper braids provided thermal contact to the cold head of the cooler and offered some compensation from the periodic length modulation occurring in the cooler due to pressure oscillation in the tubes [14].

The angular range of the stage was limited to about  $90^\circ$  by the He pressure lines connecting the cooler to the stationary compressor, but this was sufficient for the purpose of the experiment. A rotation period 10 min was chosen for a rotation over  $[0^\circ, 90^\circ, 0^\circ]$ . Faster rotation led to disturbances.

The cavities are high-reflection coated for wavelengths around  $1 \mu\text{m}$ . In order to avoid rotation-induced variations

in the alignment of the laser beams with respect to the cavities that would result in lock errors, the laser waves are brought to the cavities through two optical fibers. Two diode-pumped monolithic Nd:YAG (yttrium aluminum garnet) lasers were locked to the two cavities by means of a Drever-Hall reflection locking scheme [15]. The respective photodiodes were located in the cryostat, next to the cavities. The lasers were frequency modulated using the piezo actuators glued to the laser crystals as modulators, adding the modulation frequencies to the control feedback signals [16]. Parts of the laser beams were superimposed on a fast photodiode producing a heterodyne signal at the beat frequency  $\nu_1 - \nu_2$  between the two lasers (of the order of 700 MHz). That was measured with a frequency counter.

The periodic pressure modulation (at 1.1 Hz) led to a residual modulation of the beat frequency between the two cavity-locked lasers, which amounted to approximately 200 Hz amplitude. However, this modulation was later removed using Fourier filtering. The typical Allan standard deviation of the beat frequency (for nonrotating resonators) was 2.5 Hz for an integration time of 30 s, and 5 Hz ( $\approx 2 \times 10^{-14}$ ) for an integration time of 300 s (half of the rotation period).

The dependence of the cavity resonance frequencies on the beam powers was measured to be  $\sim 8$  Hz per  $\mu\text{W}$  impinging on the cavities. The laser powers were actively stabilized using acousto-optical modulators (AOM), also serving as optical isolators. At a typical working power of 50–100  $\mu\text{W}$  onto the cavities, the influence of residual power changes was thereby reduced to the level of 0.1 Hz ( $0.4 \times 10^{-15}$ ) for integration times of hundreds of seconds.

The dependence of the beat frequency on the temperature of the baseplate supporting the cavities was on the order of 1.5 Hz/mK.

Active stabilization resulted in an instability of 45  $\mu\text{K}$  at 300 s integration time, and thus a temperature-induced beat frequency instability on the order of 0.07 Hz ( $2 \times 10^{-16}$ ).

The sensitivity of the beat frequency to tilt of the table supporting the apparatus was 0.06 Hz/ $\mu\text{rad}$  ( $2 \times 10^{-16}/\mu\text{rad}$ ). The tilts along the two horizontal axes were monitored continuously during the rotations for later decorrelation. Typical tilt modulation during a rotation was 50  $\mu\text{rad}$  peak to peak, corresponding to a inferred beat modulation of several hertz. However, for the data analysis only the beat frequency modulation components at  $2\theta$  are relevant; for these the inferred peak-to-peak amplitudes were typically less than 1 Hz.

#### IV. RESULTS

The data analyzed in this paper were collected during very stable operation from 4 February 2005 to 8 February 2005 for 76 h. Frequency sampling was at 1-s intervals. The measured tilts were time averaged, weighted with the measured beat frequency sensitivities and subtracted from the beat data. Then, the beat modulation at 1.1 Hz, caused by the PTC, was removed. After removal of clearly disturbed rotations, the remaining 432 rotation periods  $\theta = [0^\circ; 90^\circ; 0^\circ]$  (labeled by  $i$ ) were each least-squares fitted with functions

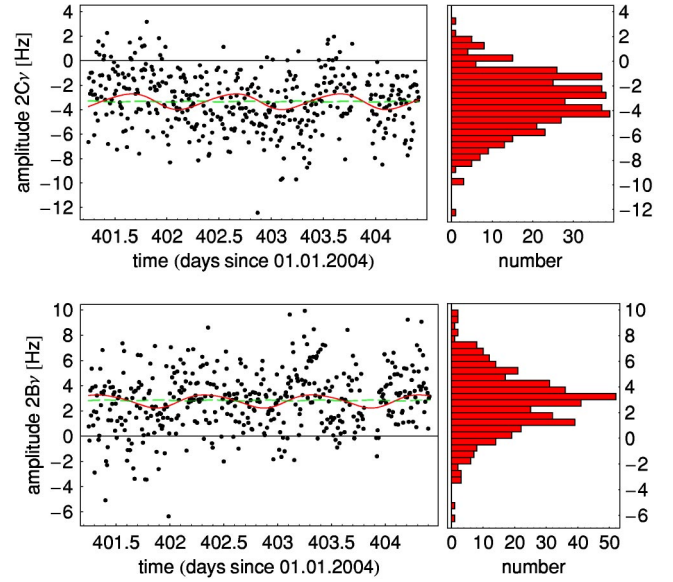


FIG. 2. Measured  $2B\nu$  and  $2C\nu$  amplitudes of spatial anisotropy for individual rotations and corresponding histograms. The fit error for each data point is less than 1 Hz. Full line: the SME model plus systematic effect. Dashed line: the RMS model plus systematic effect. Mean values:  $\langle 2B \rangle = 2.8$  Hz,  $\langle 2C \rangle = -3.3$  Hz.

$a_i t + 2B(t_i) \sin 2\theta(t) + 2C(t_i) \cos 2\theta(t)$ , where the coefficients  $a_i$  quantify a (slowly varying) linear drift.

The obtained amplitude sets  $\{2B(t_i)\}$ ,  $\{2C(t_i)\}$  are shown in Fig. 2. The data were analyzed in the following ways:

(i) Within the RMS framework, for two orthogonal cavities located on Earth and considering the preferred frame mentioned above, the beat frequency can be written as in Eq. (1) with

$$2C(t) = (1/2 - \beta + \delta)(v^2/c_0^2)(\gamma_0 + \gamma_1 \cos \omega_\oplus T_\oplus + \gamma_2 \cos 2\omega_\oplus T_\oplus + \sigma_1 \sin \omega_\oplus T_\oplus + \sigma_2 \sin 2\omega_\oplus T_\oplus),$$

$$2B(t) = (1/2 - \beta + \delta)(v^2/c_0^2)(\gamma_3 \cos \omega_\oplus T_\oplus + \gamma_4 \cos 2\omega_\oplus T_\oplus + \sigma_3 \sin \omega_\oplus T_\oplus + \sigma_4 \sin 2\omega_\oplus T_\oplus), \quad (3)$$

where  $\gamma_0 = \sin^2 \chi (3 \cos^2 \Theta - 1)/4$ ,  $\gamma_1 = (1/2) \cos \Phi \sin 2 \times \Theta \sin 2\chi$ ,  $\gamma_2 = \cos 2\Phi \cos^2 \Theta (\cos 2\chi - 3)/4$ ,  $\gamma_3 = \sigma_3 \tan \Phi$ ,  $\gamma_4 = -\sigma_4 \tan 2\Phi$ ,  $\sigma_1 = \gamma_1 \tan \Phi$ ,  $\sigma_2 = \gamma_2 \tan 2\Phi$ ,  $\sigma_3 = \cos \Phi \sin \chi \sin 2\Theta$ ,  $\sigma_4 = \cos^2 \Theta \cos \chi \cos 2\Phi$ .

$T_\oplus$  is the time since the beginning of the data plus an offset that accounts for a time difference since the coincidence of the lab's  $y$  axis with the  $\hat{Y}$  axis of the sun-centered system [9]. The direction of the sun's velocity  $\vec{v}$  relative to the cosmic microwave background is given by the right ascension  $\Phi = 168^\circ$  and the declination  $\Theta = -6^\circ$ . In fitting the above expression to our data, we take into account that the finite average values of  $2B$  and  $2C$  are likely to be due to a (constant) systematic error. We model this by adding a contribution  $b_{\text{sys}} \sin 2\theta + c_{\text{sys}} \cos 2\theta$  to Eq. (1), and fit  $b_{\text{sys}}$ ,  $c_{\text{sys}}$ ,  $\beta - \delta - \frac{1}{2}$ . Effectively, this means that only the modulation of the  $\{2B, 2C\}$  amplitudes by Earth's rotation contributes to the fit result for  $\beta - \delta - \frac{1}{2}$ .

TABLE I. Fourier amplitudes determined from the experiment. All quantities are in units of  $10^{-16}$ .

	Basis	Value	Statistical error	Systematic error
$C_0$	1	-59	3.4	3
$C_1$	$\sin(\omega_{\oplus}T_{\oplus})$	-3	1.5	0.5
$C_2$	$\cos(\omega_{\oplus}T_{\oplus})$	11	2	0.5
$C_3$	$\sin(2\omega_{\oplus}T_{\oplus})$	1	2	0.5
$C_4$	$\cos(2\omega_{\oplus}T_{\oplus})$	0.1	2	0.2

The fit yields  $\beta - \delta - \frac{1}{2} = (+0.5 \pm 3) \times 10^{-10}$  and is shown in Fig. 2. Due to the experimental error in the determination of the tilt sensitivities there is an additional (systematic) error of  $\pm 0.7 \times 10^{-10}$ . Our result is about a factor of 10 lower than the previous best results  $(-1.2 \pm 1.9 \pm 1.2) \times 10^{-9}$  [17] and  $(-2.2 \pm 1.5) \times 10^{-9}$  [6].

(ii) Using all our data we can obtain a fit of the five Fourier amplitudes of  $2C(t^*)$  at the time  $t^* \simeq 6$  February 2005 (see Table I). These amplitudes are linear combinations of the  $\tilde{\kappa}_{e-}$  and  $\tilde{\kappa}_{o+}$  coefficients, where the weights of the latter depend on Earth's orbital phase (see Appendix E of [9]). For the fit we make use of the approximate relationship between the functions  $B(t)$  and  $C(t)$  [18] and we include a coefficient  $b_0$  in  $B(t)$  in order to describe a systematic effect. Note that due to the limited extent of the data over time, the frequencies  $\omega_{\oplus} + \Omega_{\oplus}$  and  $\omega_{\oplus} - \Omega_{\oplus}$  cannot be distinguished and therefore it is not possible to extract the individual coefficients  $\tilde{\kappa}_{e-}$  and  $\tilde{\kappa}_{o+}$  from the  $C_i$  coefficients.

(iii) The results of the microwave cryogenic experiment [7] found the elements of  $(\tilde{\kappa}_{e-})$  [except for  $(\tilde{\kappa}_{e-})^{ZZ}$ ] and the elements of  $\beta_{\oplus}$  ( $\tilde{\kappa}_{o+}$ ) to be zero within several parts in  $10^{-15}$ . If we assume these elements to be zero, we can use only the  $C_0$  coefficient to determine  $(\tilde{\kappa}_{e-})^{ZZ}$ , i.e., Eq. (2) is truncated at the first term. The result is  $(\tilde{\kappa}_{e-})^{ZZ} = (-2.0 \pm 0.2) \times 10^{-14}$ . As this nonzero value is likely due to a systematic effect,

we may state that the value of  $|(\tilde{\kappa}_{e-})^{ZZ}|$  is probably less than  $2 \times 10^{-14}$ .

We believe the nonzero averages of the  $2B$  and  $2C$  amplitudes are due to a systematic effect of thermal origin. A (small) thermal gradient is present in the laboratory, through which the apparatus rotates. The magnitude of the effect is consistent with our measured temperature sensitivity and the temperature modulation amplitude measured at the top of the apparatus.

Overall, our experiment is limited firstly by the slow maximum rotation speed allowed by the system. A faster, variable rotation speed would, in principle, allow a more detailed study of the systematic effects or a partial suppression thereof. However, faster rotation could not be used with our setup. Secondly, the laser frequency lock stability is limited by the small signal-to-noise ratio (low cavity throughput), which limits the ability to more precisely characterize the systematic effects.

In conclusion, we have described a Michelson-Morley-type experiment that has led to the first determination of a limit for  $(\tilde{\kappa}_{e-})^{ZZ}$  of the standard model extension,  $|(\tilde{\kappa}_{e-})^{ZZ}| < 2 \times 10^{-14}$ . An analysis of the data in the RMS framework yielded an upper limit for a hypothetical direction dependence of  $c$  an order of magnitude lower than the best previous measurements. We note that the present results were achieved using a measurement duration 100 times shorter. The accuracy of the experiment appears to be limited by a thermal systematic effect. A significant improvement of our results would require major modifications to the apparatus.

## ACKNOWLEDGMENTS

We thank L. Haiberger for contributions to the cryostat development, A. Nevsky and C. Lämmerzahl for discussions, and G. Thummes for his helpful assistance. P.A. acknowledges the support of the DAAD, M.O. the Heinrich-Hertz Foundation. This research was part of the Gerhard-Hess Program of the German Science Foundation.

- 
- [1] C. M. Will, *Theory and Experiment in Gravitational Physics* (Cambridge University Press, Cambridge, 1993).
- [2] *Proceedings of the Meetings on CPT and Lorentz Symmetry*, edited by V. A. Kostelecký (World Scientific, Singapore, 1999 and 2002), Vols. I and II.
- [3] A. Brillat and J. L. Hall, *Phys. Rev. Lett.* **42**, 549 (1979).
- [4] P. Wolf *et al.*, *Phys. Rev. Lett.* **90**, 060402 (2003).
- [5] J. A. Lipa *et al.*, *Phys. Rev. Lett.* **90**, 060403 (2003).
- [6] H. Müller *et al.*, *Phys. Rev. Lett.* **91**, 020401 (2003).
- [7] P. Wolf *et al.*, *Phys. Rev. D* **70**, 051902(R) (2004).
- [8] R. Mansouri and R. Sexl, *Gen. Relativ. Gravit.* **8**, 497 (1977).
- [9] V. A. Kostelecký and M. Mewes, *Phys. Rev. D* **66**, 056005 (2002).
- [10] V. A. Kostelecký and M. Mewes, *Phys. Rev. Lett.* **87**, 251304 (2001).
- [11] M. E. Tobar *et al.*, *Phys. Rev. D* **71**, 025004 (2005).
- [12] H. Müller *et al.*, *Int. J. Mod. Phys. D* **7**, 1101 (2002).
- [13] C. Wang *et al.*, *Cryogenics* **37**, 159 (1997).
- [14] C. Lienherth *et al.*, *IEEE Trans. Appl. Supercond.* **11**, 812 (2001).
- [15] R. Drever *et al.*, *Appl. Phys. B: Photophys. Laser Chem.* **31**, 97 (1983).
- [16] G. Cantatore *et al.*, *Rev. Sci. Instrum.* **66**, 2785 (1995).
- [17] P. Wolf *et al.*, *Gen. Relativ. Gravit.* **36**, 2352 (2004).
- [18] The Fourier amplitudes of the  $B$  data can be obtained from the  $C$  amplitudes if the contributions due to the velocity of the laboratory with respect to the Earth's center,  $\beta_L \approx 10^{-6}$ , are neglected. Then  $B_0=0$ ,  $B_1=-C_2/\cos \chi$ ,  $B_2=C_1/\cos \chi$ ,  $B_3=-2C_4 \cos \chi/(1+\cos^2 \chi)$ , and  $B_4=2C_3 \cos \chi/(1+\cos^2 \chi)$ .